Y-Stent Coiling of Basilar Bifurcation Aneurysms Induces a Dynamic Angular Vascular Remodeling With Alteration of the Apical Wall Shear Stress Pattern

Bulang Gao, MD, PhD
Merih I. Baharoglu, MD
Alex D. Cohen, MD
Adel M. Malek, MD, PhD

Cerebrovascular and Endovascular Division, Department of Neurosurgery, Tufts Medical Center and Tufts University School of Medicine, Boston, Massachusetts

Correspondence:
Adel M. Malek, MD, PhD,
Department of Neurosurgery,
Tufts Medical Center, 800 Washington Street, #178, Proger 7,
Boston, MA 02111.
E-mail: amalek@tuftsmedicalcenter.org

Received, October 10, 2011.
Accepted, December 11, 2012.
Published Online, December 28, 2012.

Copyright © 2012 by the Congress of Neurological Surgeons

BACKGROUND: Although wide-necked basilar bifurcation aneurysms are treated with Y-stent coiling, the effect of this intervention on vessel configuration and hemodynamics is unknown.

OBJECTIVE: To investigate the immediate and delayed effects of Y-stenting using self-expanding microstents on basilar bifurcation architecture and hemodynamics.

METHODS: Fifteen patients underwent basilar Y-stent coiling and imaging with rotational angiography. Vascular angles were measured between proximal P1 segments of the posterior cerebral arteries (α) and between the basilar artery and each P1 segment ($\beta_{1,2}$) in the anteroposterior and $\gamma_{1,2}$ sagittal planes. Patient-specific computational fluid dynamic analysis was used to estimate wall shear stress (WSS) changes with treatment.

RESULTS: In the anteroposterior plane, Y-stenting significantly decreased angle α and increased β angles immediately after stent coiling ($P < .05$ and $P < .01$, respectively) in a continued dynamic remodeling that progressed further in later months; sagittal γ angles also decreased ($P < .0001$). This novel stent-induced geometric progressive remodeling resulted in effective straightening and narrowing of the basilar bifurcation angle α (150.0 degrees vs 113 degrees, $P < .0001$) with significant correlation ($r = 0.39$, $P < .05$) between pretreatment proximal P1 angles and maximal angular change. Computational fluid dynamic analysis showed the angular remodeling led to significant narrowing of the WSS interpeak at the apex, redirecting high WSS away from the neck transition zone with native vessel toward the inert coil mass.

CONCLUSION: Y-configuration stent coiling induced immediate and, more significantly, a previously undefined delayed cerebrovascular remodeling. This progressive stent-induced angular remodeling alters perianeurysmal hemodynamics, independent of the flow-diverting properties of stent struts, thus shifting the balance of hemodynamic forces affecting aneurysm development and evolution.

KEY WORDS: Angular modification, Basilar bifurcation, Computational fluid dynamics, Intracranial aneurysm, Stent-assisted coiling, Vascular remodeling, Wall shear stress

Neurosurgery 72:617–629, 2013 DOI: 10.1227/NEU.0b013e3182846d9f www.neurosurgery-online.com

Conventional unassisted endovascular coiling of wide-necked cerebral aneurysms is often impossible because of the risk of coil herniation and, when attempted, often results in subtotal packing leading to aneurysm recurrence. Intracranial self-expanding stents have been increasingly used as adjuncts to provide a mechanical scaffold to buttress the coils across the neck of these wide-necked lesions with increasing success.[1-5] Since their introduction, intracranial self-expanding stents have not only been used for sidewall aneurysm coiling, but also increasingly deployed in various single or double configurations for stent coiling of wide-necked bifurcation aneurysms.[1-5] These include the double sequential

ABBREVIATIONS: BA, basilar artery bifurcation; **CFD,** computational fluid dynamics; **3-D–RA,** 3-dimensional rotational angiography; **ICA,** internal carotid artery; **IEL,** internal elastic lamina; **WSS,** wall shear stress

Copyright © Congress of Neurological Surgeons. Unauthorized reproduction of this article is prohibited.

deployment in a Y configuration or "kissing" fashion from the parent vessel into each of the daughter branches (Figure 1A), as well as the transcirculation deployment of a horizontal stent across the neck of the aneurysm via the anterior or posterior communicating artery.

Unlike the fixed-radius, balloon-mounted coronary stents first described for stent-mediated aneurysm coiling,[6] the current generation of self-expanding intracranial microstents used for stent-mediated coiling includes the Neuroform stent (Boston Scientific Corp, Natick, Massachusetts) and the Enterprise Vascular Reconstruction Device (Codman Neurovascular, Raynham, Massachusetts). These are constructed of shape-memory nickel-titanium alloy (nitinol) and exert a continuous outwardly

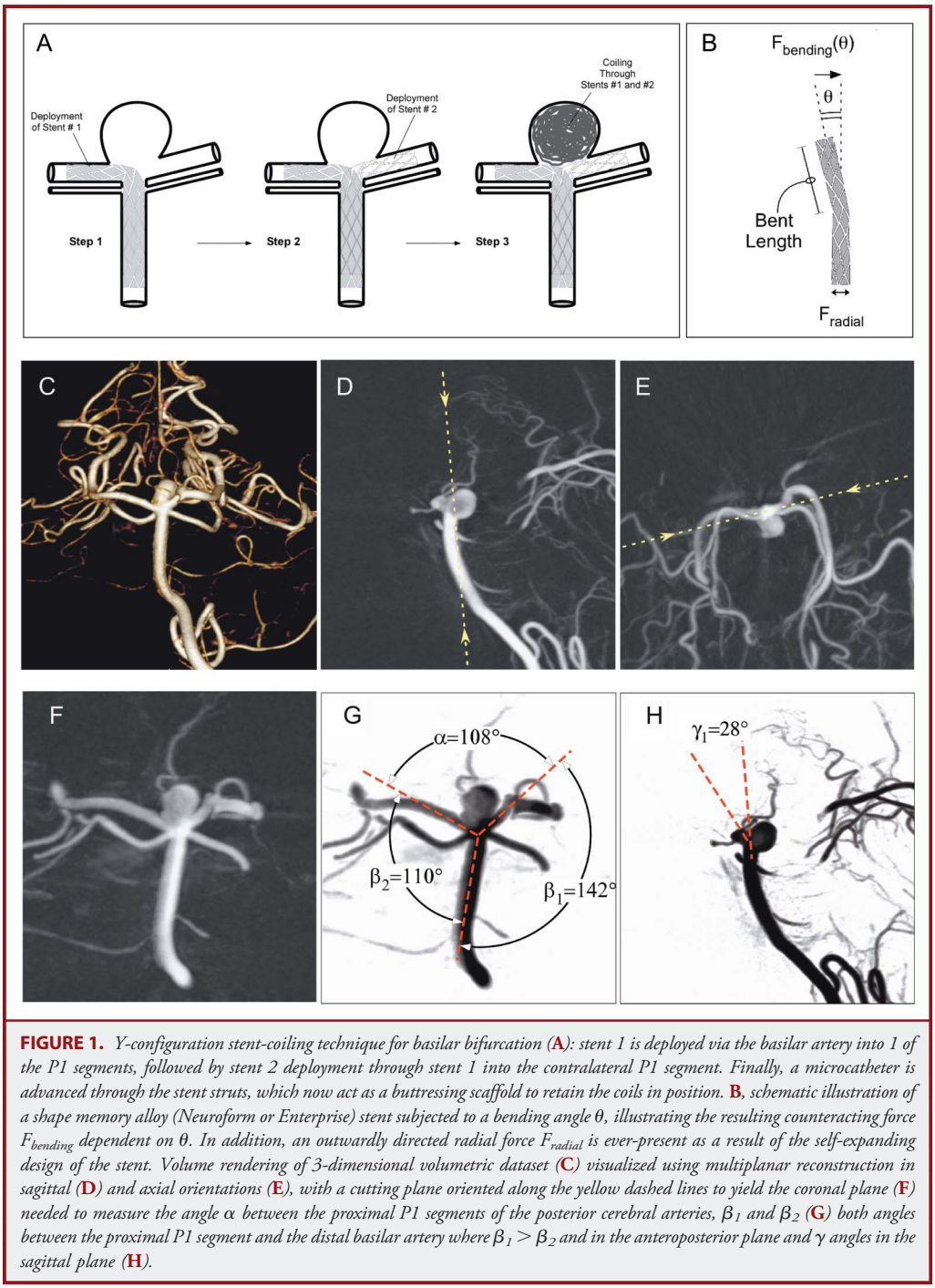


FIGURE 1. *Y-configuration stent-coiling technique for basilar bifurcation (**A**): stent 1 is deployed via the basilar artery into 1 of the P1 segments, followed by stent 2 deployment through stent 1 into the contralateral P1 segment. Finally, a microcatheter is advanced through the stent struts, which now act as a buttressing scaffold to retain the coils in position. **B**, schematic illustration of a shape memory alloy (Neuroform or Enterprise) stent subjected to a bending angle θ, illustrating the resulting counteracting force $F_{bending}$ dependent on θ. In addition, an outwardly directed radial force F_{radial} is ever-present as a result of the self-expanding design of the stent. Volume rendering of 3-dimensional volumetric dataset (**C**) visualized using multiplanar reconstruction in sagittal (**D**) and axial orientations (**E**), with a cutting plane oriented along the yellow dashed lines to yield the coronal plane (**F**) needed to measure the angle α between the proximal P1 segments of the posterior cerebral arteries, β_1 and β_2 (**G**) both angles between the proximal P1 segment and the distal basilar artery where $\beta_1 > \beta_2$ and in the anteroposterior plane and γ angles in the sagittal plane (**H**).*

Copyright © Congress of Neurological Surgeons. Unauthorized reproduction of this article is prohibited.

directed radial force (Figure 1B). In addition, these stents exert a mild force in resisting bending motion and have been previously described to induce in-stent stenosis in a certain proportion of patients.[7]

Following the observation of a bifurcation angular change during routine follow-up angiography, we sought to systematically evaluate the effect of intracranial Y-stenting for treatment of wide-necked aneurysms at the basilar artery bifurcation (BA) using high-resolution, 3-dimensional (3-D) rotational angiography (3-D–RA). We hypothesized that intracranial stenting using self-expanding shape-memory alloy stents may lead to long-term alteration in the vascular bifurcation in which they are deployed. We also sought to evaluate the hemodynamic changes caused by Y-stenting using computational fluid dynamic (CFD) analysis of patient-specific data, trying to delineate changes in the hemodynamic factors that have been previously implicated in the initiation and progression of intracranial aneurysms and their implications to the process of aneurysm development and recurrence.

PATIENTS AND METHODS

Patient Population and Treatment Method

Between March 2003 and February 2011, 15 patients (13 women and 2 men) with an age range of 37 to 80 years (mean, 58 years), underwent Y-stenting for coil embolization of 15 wide-necked BA aneurysms after providing informed consent. The symptoms included acute subarachnoid hemorrhage in 3 patients, a history of subarachnoid hemorrhage in 5, headache in 2, syncope and confusion in 1, hand numbness in 1, and transient ischemic attack in 1. The remaining 2 patients were incidentally found. In 13 patients, Neuroform stents were inserted into each P1 daughter vessel, and in 2 patients, an Enterprise stent was used to cross an initial Neuroform stent to form the Y-construct because tortuosity at the basilar-posterior cerebral artery junction prevented navigation of the 0.027 in the Neuro Renegade (Boston Scientific) microcatheter required for Neuroform stent deployment. This retrospective study was approved by the hospital's institutional review board.

Stent-Assisted Coiling Procedure and Angiographic Follow-up Protocol

Patients were placed on an antiplatelet regimen consisting of clopidogrel bisulfate 75 mg/d and acetylsalicylic acid 325 mg/d beginning at least 3 to 5 days before and treated under general endotracheal anesthesia and intravenous anticoagulation with heparin to an activated clotting time of 230 to 250 s.

Coiling was performed in the same session after stenting in 11 patients. Four patients were managed with coiling first and then stent coiling for aneurysm recurrence at later angiographic follow-up. All these patients routinely underwent 3-D–RA before and immediately after stent coiling and at each angiographic follow-up. Patients routinely underwent an early follow-up angiogram at 3 to 6 months post-procedure to monitor for risk of basilar in-stent stenosis given the double-stent overlap in that segment.[7-9] A 3-T magnetic resonance angiogram was obtained contemporaneously with the catheter angiogram to serve as baseline and enable noninvasive comparison and long-term monitoring.

3-D Modeling and Vascular Angle Measurement

Biplane 2-dimensional digital subtraction angiography and 3-D–RA were performed on the identical Siemens Axiom-Artis VB22N unit in all cases. 3-D–RA volumetric acquisitions were reconstructed and transferred for 3-D analysis to the Amira 4.1.2 software package (Visage Imaging, San Diego, California). After orthogonal orientation of the target bifurcation, 3 vascular angles α, β_1, and β_2 were measured (Figure 1) in the anteroposterior plane as follows: α representing the basilar bifurcation angle measured between the proximal P1 segments of the posterior cerebral arteries and β_1 and β_2 corresponding to the angle between the basilar artery and each proximal P1 segment where $\beta_1 > \beta_2$ by convention. Multiplanar reconstructions were oriented at the basilar tip to be aligned with the distal basilar artery in the sagittal plane and to the bilateral proximal P1 segments in the axial plane, yielding the orthogonal plane (Figures 1F and 1G), which enabled the measurements of the angles (α, β_1, and β_2). In the sagittal plane (Figure 1H), lateral angles of each P1 segment deviating from the plane where distal basilar artery was located were measured as γ_1 and γ_2, where $\gamma_1 > \gamma_2$ by convention. Angles were measured using this method before and after stent coiling and at subsequent angiographic follow-up studies.

Computational Fluid Dynamics and Postprocessing

CFD analysis was performed using the patients' 3-D–RA data before stenting and at the latest angiographic follow-up for comparison of hemodynamic alteration caused by angular remodeling. Surface smoothing of the 3-D reconstructed datasets was performed using the MeshLab software (MeshLab versions 1.2.2, Visual Computing Lab, Istituto di Scienza e Tecnologie dell'Informazione, Consiglio Nazionale delle Ricerche). Virtual removal of the aneurysm and surface reconstruction of the aneurysm neck were also performed using the MeshLab software. High-resolution polyhedral meshes were generated with Star-CCM+ Version 4.02 (CD-Adapco, Melville, New York) at a count of approximately 1 000 000 cells. Finite-volume solution used Fluent Version 6.3.26 (Ansys, Lebanon, New Hampshire) in a laminar double-precision unsteady regimen, assuming rigid nonslip wall conditions, blood viscosity of 3.5 cP, and density of 1070 kg/m^3, as previously described.[10] Postprocessing was performed using the Ensight software package (Version 9; CEI, Apex, North Carolina).

Statistics

Statistical analysis was performed using matched paired *t* tests and linear regression analysis using JMP software (Version 8.02; SAS Institute, Cary, North Carolina). Significance was assumed for a value of $P < .05$.

RESULTS

Angular Remodeling

Aneurysm size ranged from 1.6 to 16 mm (mean, 6.9 mm) and the neck from 2.7 to 6.7 mm (mean, 5 mm) (Figures 2 and 3). Thirty stents in total were deployed in these patients, with 28 Neuroform stents (6 measuring 3 × 15 mm, 16 measuring 3.5 × 15 mm, 4 measuring 3.5 × 20 mm, 2 measuring 4 × 15 mm) and 2 Enterprise stents (measuring 4.5 × 22 mm).

All patients underwent angiographic follow-up from 1 to 48 months (mean, 13 months) after the stent-coiling procedure. Fifteen patients completed the *early* angiographic workup between

Copyright © Congress of Neurological Surgeons. Unauthorized reproduction of this article is prohibited.

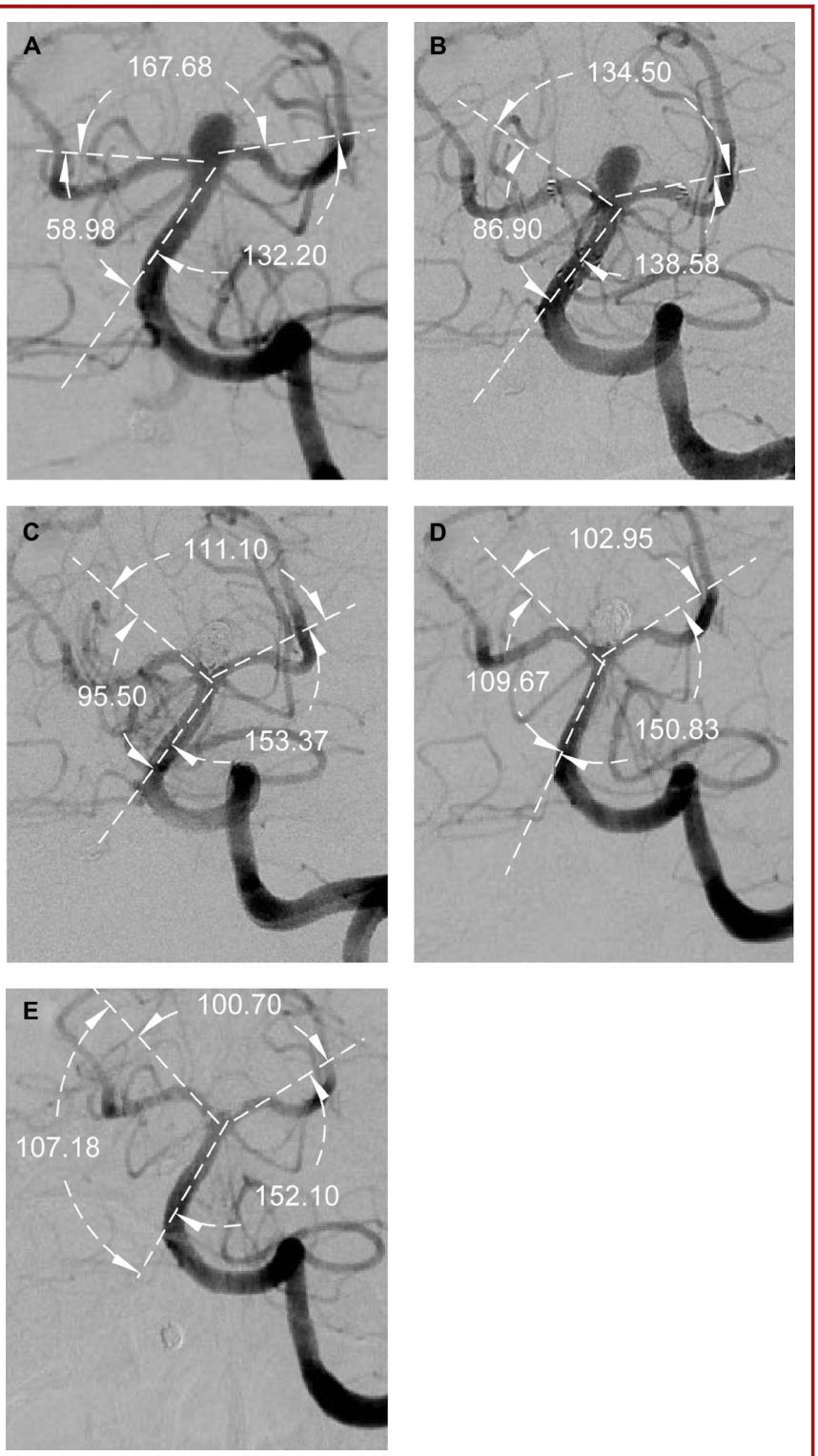


FIGURE 2. *A 64-year-old woman had a wide-necked 7 mm basilar tip aneurysm, and pre-treatment angle α was 167.7° (A). Immediately following Y-stenting, angle α changed to 134.5° (B). After coiling, angle α was measured at 111.1° (C). Four months later, angle α was 103° (D) and at 12-month follow-up, angle α was 100.7° (E).*

Copyright © Congress of Neurological Surgeons. Unauthorized reproduction of this article is prohibited.

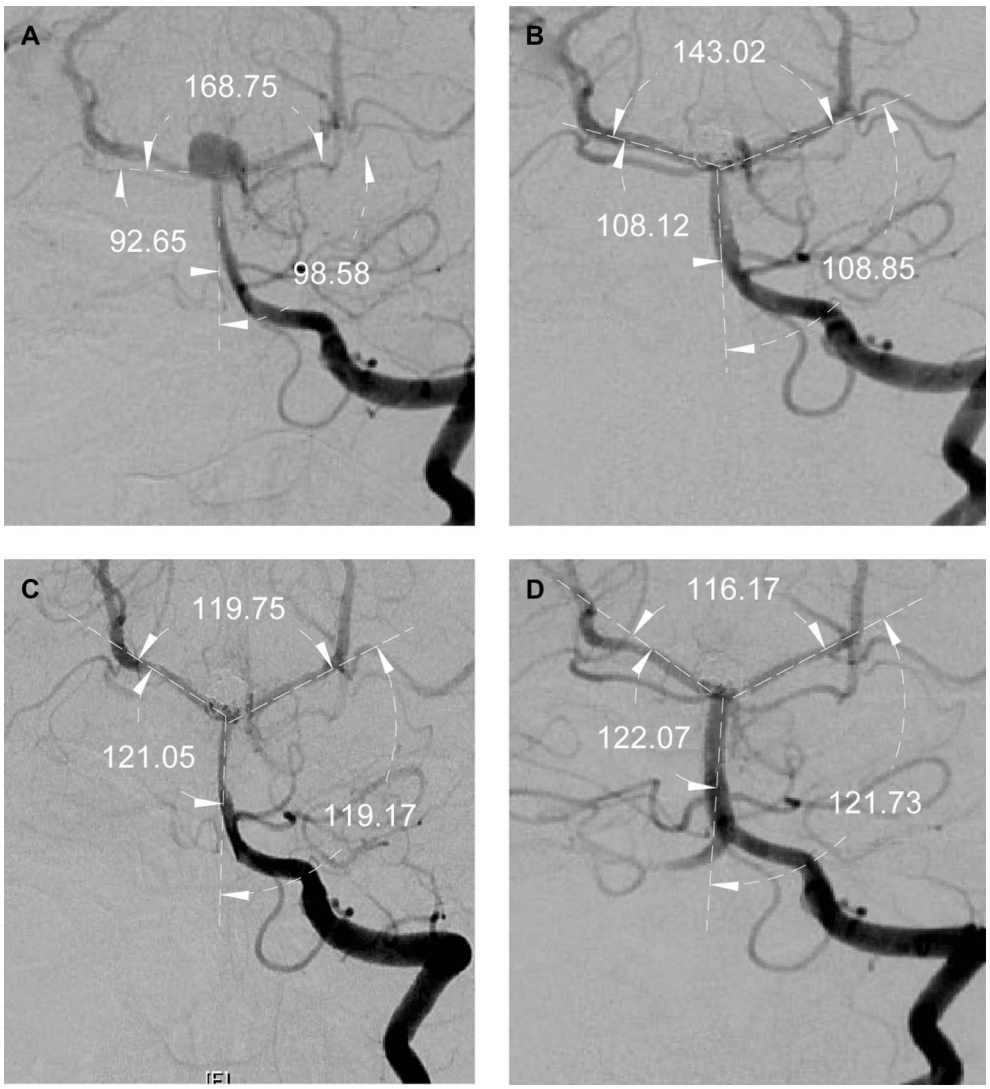


FIGURE 3. *A 45-year-old woman had a wide-necked 6 mm basilar tip aneurysm, with pre-treatment angle α of 168.8° (A). Following Y-type stenting and coiling, angle α changed to 143.0° (B). At 4-month follow-up, angle α was 119.8° (C) and twelve months later, angle α was 116.2° (D).*

1 and 7 months (mean, 3.5 months) after the procedure, and 8 patients underwent the *late* angiographic follow-up between 10 and 48 months (mean, 18.9 months) after stent coiling (Figures 2 and 3). No new symptoms related to vascular remodeling were found at follow-up studies.

In the anteroposterior plane, α ranged from 116 degrees to 197.3 degrees (mean, 150.0 degrees), β_1 ranged from 102.9 degrees to 137.5 degrees (mean, 119.8 degrees), and β_2 ranged from 59 degrees to 119 degrees (mean, 93.7 degrees) before stenting (Table 1). At the end of the stent-coiling procedure, α decreased to between 93 degrees to 135 degrees (mean, 134.7 degrees), whereas β_1 increased to between 91 degrees to 159 degrees (mean, 124.4 degrees) and, similarly, β_2 increased to between 109 degrees to 143 degrees (mean, 105.8 degrees). Compared with before stenting, a significant ($P < .05$) or highly significant difference ($P < .01$) existed in all the angles in the anteroposterior plane at the end of stent coiling and at the early and late angiographic follow-ups (Table 1). At late follow-up, angle α continued to decrease, with a significant difference ($P < .05$), compared with early follow-up. No significant differences ($P > .05$) were found between early and late follow-up at angles β_1 and β_2. The results were also analyzed in a fractional manner with respect to the angular changes and different times before and after stenting and at follow-up (Figure 4A).

Copyright © Congress of Neurological Surgeons. Unauthorized reproduction of this article is prohibited.

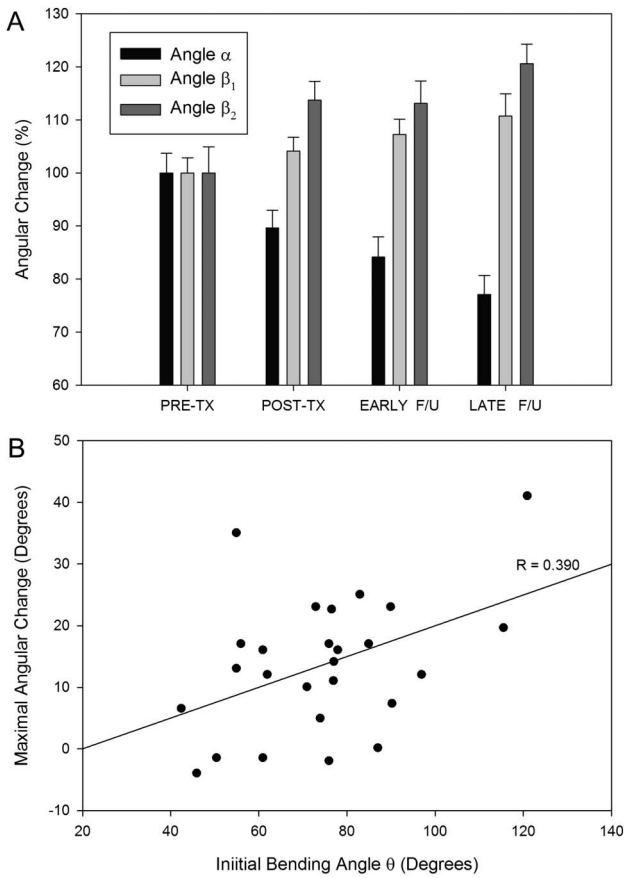


FIGURE 4. *Percent changes in the mean value of anteroposterior angles (α, β_1, β_2) in Y stent-coiling at different time points (**A**). The percent changes in basilar bifurcation angle α decreased significantly, while those in angles β_1 and β_2, between the basilar artery and its P1 branches (P1-BA), increased significantly. (TX: treatment; F/U: follow-up). (**B**) Regression analysis between the pre-treatment stent bending angle (θ = 180-β_1 or 180-β_2) at each P1-BA instance and the angular difference between pre-treatment and latest follow-up at angles β_1 and β_2 in Y-stent cases. The maximal angular change indicates the angle change caused by Y-stenting at the latest follow-up compared with pre-treatment. The initial stent bending angle indicates the angle of a stent being bent if it is deployed in place and equals 180-β_1 or 180-β_2. A positive correlation exists between the maximal angular change and the bending angle (θ), indicating the greater the initial bending angle, the greater the maximal angular change at latest follow-up.*

In the sagittal plane, γ_1 ranged from 12.2 degrees to 35.3 degrees (mean, 17.9 degrees) and γ_2 from 6.8 degrees to 23 degrees (mean, 12.8 degrees) before stenting (Table 1). At latest follow-up, γ_1 decreased to between 3 degrees and 17.4 degrees (mean, 9.6 degrees) and γ_2 decreased to between 3.8 degrees and 14 degrees (mean, 7.9 degrees), both with a highly significant difference ($P < .0001$) compared with before stenting.

Analysis of the initial bending angle (θ = 180-β_1, or 180-β_2) before stenting and at the latest follow-up demonstrated a linear correlation (r = 0.39, $P < .05$) between θ and the maximal angular change between before treatment and at latest follow-up in the angle between the proximal P1 segments and the basilar artery ($\beta_{1,2}$) (maximal angle change $-4.97 + 0.249 * \theta$) (Figure 4B).

CFD Estimation of Remodeling Effect

To evaluate the isolated effect of the angular change induced by stenting, a neck-capping technique was necessary because stent deployment induced an immediate angular change (Figure 5A). This enabled the comparison of the hemodynamics in all bifurcations between the capped (Figure 5B) and latest follow-up (Figure 5C) configurations. CFD analysis was coupled with cut plane along the basilar apex from 1 P1 to its counterpart (Figure 5D and 5E) to enable analysis of the wall shear stress (WSS) profiles from all patient-specific reconstructions.

Analysis of the pressure and velocity patterns in the coronal plane of the basilar artery and its bifurcation was possible and enabled evaluation of the isolated effect of Y-stenting (Figure 6). Blood flow directly impinged the basilar apex wall, with the impinging zone on the wall greater at the capped pretreatment (simulating virtual coiling) configuration (Figure 5 and 6, left panels) than at latest follow-up (Figures 5 and 6, right panels). At the center of the impinging zone (Figure 6, arrow), the flow is perpendicular to the apex wall where the pressure is the greatest, whereas the WSS is the least. At both sides of the impinging center, which serves as the flow divider, the flow changes its direction, forming the secondary flow to enter both P1 segments, and the alteration of flow direction was over a greater distance with decreased persistence of disturbed flow after stent-induced angular narrowing. As flow changed its direction, sped up, and returned to laminar flow from disturbed flow, the pressure decreased rapidly from its peak value, whereas the WSS abruptly increased from the minimal value to its peak (Figure 7).

The flow stagnation zone at the bifurcation apex was consistently seen to be diminished at the latest angiographic follow-up (Figure 6C). The blue area on top of the basilar apex wall (Figure 6, arrow) delineates very low flow velocity and was the center of the impinging blood flow stagnation region, corresponding to the maximal pressure and the minimal WSS on the basilar apex wall. This area was decreased at follow-up compared with after aneurysm removal (Figure 7B).

The pressure was primarily higher on the apex of the basilar bifurcation, mostly deviating toward the P1 branch forming the larger angle with the basilar trunk (Figure 7A). At follow-up when the bifurcation angle became smaller, the pressure became mainly focused on the bifurcation apex but with sharper fall off and decreased extent (Figure 7A).

Evaluation of the WSS profile across the basilar apex revealed the presence of 2 WSS peaks (peaks 1 and 2; Figure 7B) straddling the trough at the point of impingement where the WSS is lowest. These 2 peaks of the WSS were analyzed across all treated aneurysms, along with their respective distances D1 and D2 (Table 2). Stent coiling led to a decrease in both WSS peak

Copyright © Congress of Neurological Surgeons. Unauthorized reproduction of this article is prohibited.

TABLE 1. Mean Vascular Angles Before and After Stent Coiling and at Follow-up (Mean ± SEM), Measured in 3-Dimensional Space

	Angle	Before treatment, degrees	After Stent Coiling, degrees	Early Follow-up, degrees	Late Follow-up, degrees
Anteroposterior angles	α	150.0 ± 5.7	134.7 ± 5.0[a]	126.8 ± 5.6[a,b]	113 ± 6.6[a,b,c]
	β_1	119.8 ± 3.4	124.4 ± 3.1[d]	127.9 ± 3.4[a]	131.7 ± 4.5[a,b]
	β_2	93.7 ± 4.4	105.8 ± 3.1[a]	105.3 ± 3.7[a]	115.1 ± 4.5[a,b]
Lateral angles	γ_1	17.9 ± 1.7			9.6 ± 1.1[a]
	γ_2	12.8 ± 1.3			7.9 ±0 .9[a]

[a] P <.01 or .0001 compared with prestenting.
[b] P < .01 or .0001 compared with poststent coiling.
[c] P <.05 compared with early follow-up.
[d] P < .05 compared with prestenting.

values, which was statistically significant for peak 1 (P = .034) and also showed decrease in distances to the peaks, which was highly significant for D2 and D1 + D2, showing a narrowing of the interpeak distance of 1.8 mm (P = .003). This is an important finding because the narrower impingement zone of the higher WSS values and high spatial gradient (slope of the WSS profile) induced by stenting would have the effect of moving these hemodynamic conditions previously shown to induce aneurysmal changes away from the aneurysm neck–parent vessel transition zone, where recanalization is thought to occur, to within the shaper confines of the coiled aneurysm neck which is biologically inert covered with coil loops.

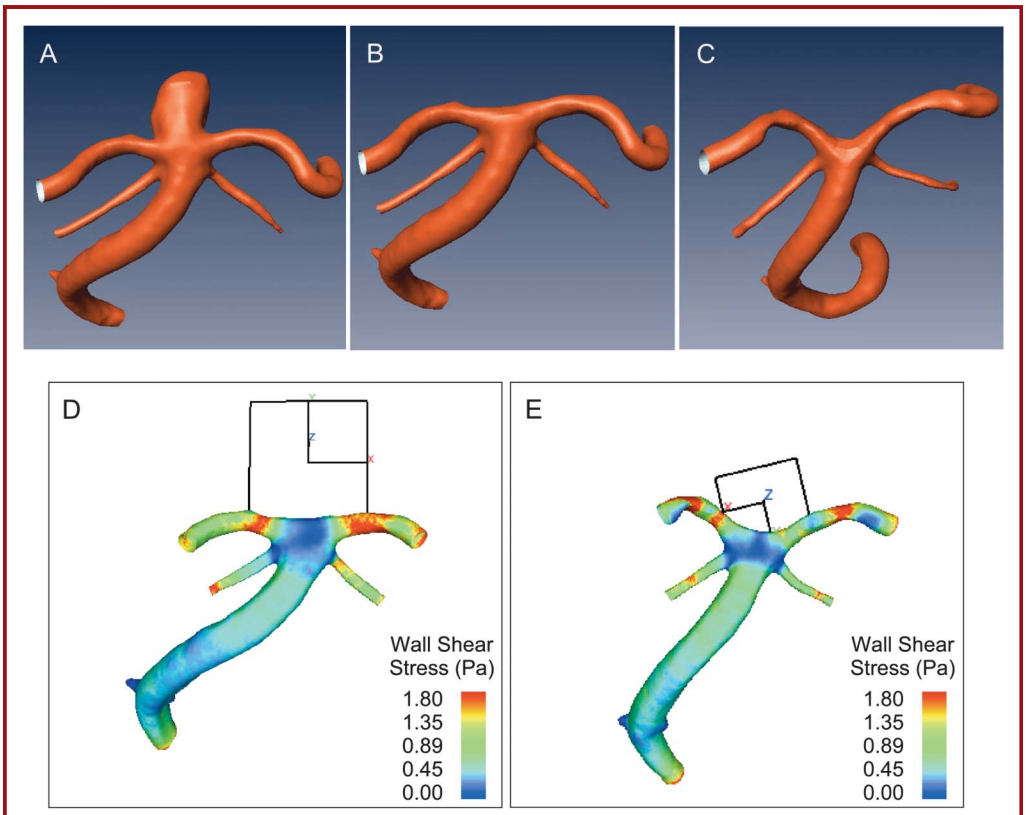


FIGURE 5. *Surface rendering of the a basilar bifurcation aneurysm before treatment (A), after dome removal (capping) to simulate non-stent-assisted virtual coiling (B), and at latest follow-up angiography after stent-coiling (C) demonstrating the stent-induced significant angular remodeling and narrowing at the bifurcation. Computational fluid dynamic analysis was performed on the preceding volumes yielding the peak-systolic wall shear stress (WSS) distribution of the capped aneurysm (D) and that after stent-coiling at latest follow-up (E). A cut-plane was used along the basilar bifurcation and P1-P1 segments to derive a WSS line-profile for subsequent analysis.*

Copyright © Congress of Neurological Surgeons. Unauthorized reproduction of this article is prohibited.

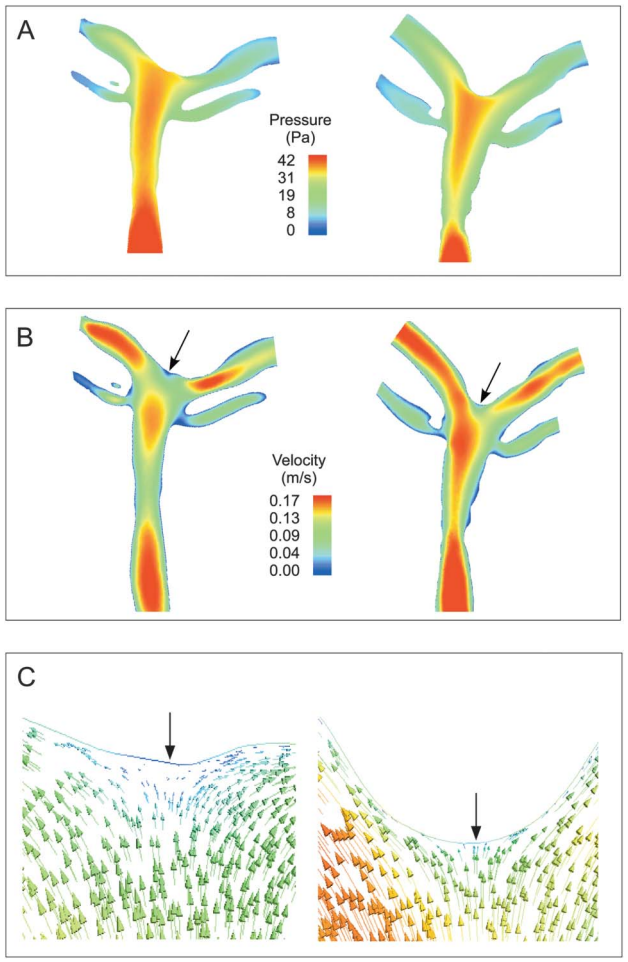


FIGURE 6. *Pressure (A) and velocity (B) cut planes along with in-plane velocity vector (C) representation of the flow-impingement zone at the apex of the basilar bifurcation showing the effect of the stent-induced angular remodeling, including a narrowing of the high-pressure flow stagnation zone (arrows).*

DISCUSSION

In this study, a novel dynamic delayed change in the vascular angles at the basilar bifurcation was uncovered in aneurysms treated with Y-stenting, a previously unknown response of the cerebrovascular circulation. Y-stenting led to a significant increase in angles β and γ but a decrease in bifurcation angle α in the anteroposterior plane at the end of the stent-coiling procedure. Furthermore, this angular change trend continued after treatment, as noted on both early and delayed follow-up. In the sagittal plane, Y-stenting also significantly decreased the deviating degree (angles of γ_1 and γ_2) of each P1 from the plane of the distal basilar artery, flattening the P1 segments and the distal basilar artery into 1 plane. This unique phenomenon was shown to have significant hemodynamic consequences at the apex of the basilar bifurcation.

The angular remodeling of the basilar bifurcation in response to Y-stenting is most likely the result of the self-straightening force countering the angle-dependent bending of the self-expanding intracranial microstents used. Zenteno et al[4,5] reported that stenting alone could change the angulation of the parent artery and facilitate thrombosis of the aneurysms at the vertebrobasilar junction, possibly by parent vessel angular modification. However, their work differed from the current data because they used balloon-mounted stents and the angular change was the immediate result of the balloon inflation–induced vessel straightening rather than a delayed vascular response resulting from the self-expanding stent. They also did not report on angular alterations caused by Y-stenting in bifurcation aneurysms. Although Canton et al[2] studied the in vitro intra-aneurysmal hemodynamic changes caused by Y-stenting in bifurcation aneurysms, these were performed in vitro and did not include the effect of any angular changes at the bifurcation.

The Neuroform and Enterprise stents used in this study are both flexible, nickel-titanium alloy (nitinol) stents specially designed for use in the cerebral vasculature.[1,3] The Neuroform stent is of open-cell design, whereas the Enterprise stent is of closed-cell design. The longitudinal stiffness of these 2 stents was recently shown to be higher in the Enterprise device[11]; nonetheless, a comparison of stent types was not possible here because only 2 Enterprise stents were used to cross a previously deployed Neuroform stent in 2 patients, an insufficient number for statistical significance. The deployment of these stents in a Y configuration significantly changed the bifurcation angles, as demonstrated at the end of the stent-coiling procedure. As time elapsed after stent deployment, the ever-present force resulting from the bending of these self-expanding shape-memory alloy stents resulted in a remodeling cerebrovascular response, leading to greater angular narrowing of the P1-P1 angle α compared with that at the end of the stent-coiling procedure, effectively straightening the vessels. It is important to note that the basilar bifurcation and the proximal P1 segments of the posterior cerebral arteries provide the origin for many critical perforator arteries, although it is unclear whether or how these vessels were affected by the angle change in the long term.

The linear correlation between θ and the maximal angular change between pretreatment and latest follow-up is consistent with the fact that the more either the Neuroform or Enterprise stent is bent, the greater is the force generated and the greater the consequent angle alteration that was observed. Additional work is needed to define the amount of force generated by these stents and to ensure that newer designs do not apply even greater forces that could have a deleterious effect on the cerebral vasculature. Finally, it remains unclear whether similar angular changes are likely to be seen in the increasingly used class of flow-diverting stents,[12] the latter having a different braided design compared with the Neuroform stent.

What effects does the shape change of the basilar bifurcation have on the local hemodynamics and consequent aneurysmal recurrence or initiation? Most research on aneurysm hemodynamics is based on

Copyright © Congress of Neurological Surgeons. Unauthorized reproduction of this article is prohibited.

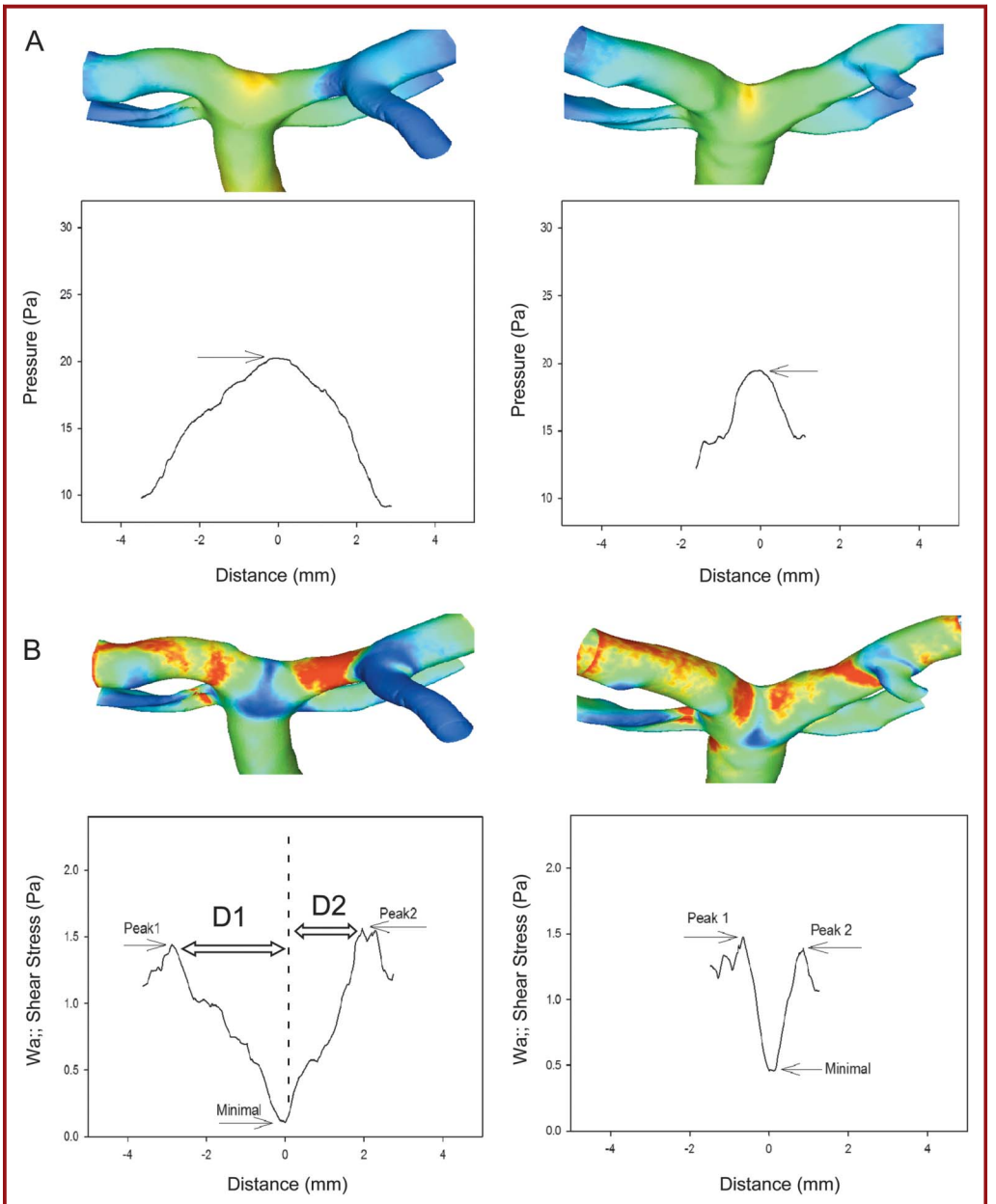


FIGURE 7. *Peak-systolic pressure (**A**) and wall shear stress (**B**) profiles before (left) and after (right) stent coiling illustrate the hemodynamic consequences of stent-induced angular remodeling. These include a narrowing of the relative high-pressure zone at the apex. More importantly, the regions of focal high wall shear stress (WSS) (peaks 1 and 2) that have been shown to colocalize with underlying destructive remodeling of the vessel wall are brought closer to the apex with decreases in apex-WSS peak distances (D1 and D2). This has the effect of moving the high WSS peak bands from the native vessel neck transition zone where destructive remodeling could lead to aneurysm regrowth and recurrence inward toward the coil mass, which is biologically inert.*

the flow alteration or deflection by the stent struts at the neck of the aneurysm and into the dome, but no information is offered on the hemodynamic alterations resulting from the angular changes of the daughter vessels that were uncovered here. The effect of the Y-stent vascular angle modification was explored here and was shown to add another potentially beneficial factor in addition to the flow-diverting features of stent struts and the in-stent stenosis, which results from the intimal hyperplastic response to stent implantation. The narrowing of the basilar bifurcation angle was in fact noted to reverse some of the pathological changes seen at the

Copyright © Congress of Neurological Surgeons. Unauthorized reproduction of this article is prohibited.

TABLE 2. Distance Between the Minimal and Peak Wall Shear Stress on the Basilar Apex Wall at Capped and Latest Follow-up Time (Mean ± SEM)[a]

Distance	Pretreatment Capped	Latest Follow-up	*P* Value
WSS peak 1, Pa	2.03 ± 0.42	1.29 ± 0.16	.034
WSS peak 2, Pa	2.29 ± 0.37	1.42 ± 0.23	.099
D1, mm	2.8 ± 0.3	2.1 ± 0.2	.066
D2, mm	3 ± 0.3	2.2 ± 0.2	.004
WSS interpeak distance D1 + D2, mm	6 ± 0.4	4.2 ± 0.3	.003

[a]WSS, wall shear stress; D1, distance between the minimal and peak 1 of WSS; D2, distance between the minimal and peak 2 of WSS (Figure 7).

apices of aneurysmal bifurcations based on the previous work of others as described in the following.

Indeed, the apex of bifurcations is the site of maximal hemodynamic stress in a vascular network. This is caused by the direct impact, deflection, and separation of the blood flow streamlines and because of vortex formation at the lateral angles.[13,14] The layer with the highest velocity of blood flow moves toward and directly impinges at the bifurcation apex where blood flow is divided. Thus, the arterial bifurcation apex experiences highly variable regions of the WSS characteristic of flow separation. Regions of an elevated WSS are believed to cause injury to the endothelial cells of the vessel wall and predispose the vessel to destructive aneurysmal remodeling.[13,15,16] Moreover, the geometry of the bifurcation helps to determine the size of the vortices formed there; these vortices tend to be larger if the combined size of the daughter vessels is much larger than the parent artery, if the bifurcation angle is large, or if the daughter arteries are curved.[13] The tensile or stretching forces of the arterial bifurcation affecting disease formation at the apex may also be determined by the bifurcation angle.[13] In addition to the kinetic energy imparted to the bifurcation apex, there is also accompanying flow turbulence that forms flow eddies and vortices to damage the vascular wall.[13] Roach et al[17] studied the hemodynamic importance of the bifurcation geometry in the circle of Willis and found that the bifurcation angle could affect the formation of flow turbulence near the bifurcation apex. Brown[18] studied the geometry of arterial bifurcations and reported that the transmural pressure in the smaller daughter branch is greater than or equal to that in the larger daughter branch and that the larger daughter branch makes a smaller angle with the direction of the parent artery. Change in the shape of the bifurcations during the cardiac cycle, leading to loss of static equilibrium at the apex of the bifurcation and disruption of the vessel wall elements, has been proposed as the mechanism of aneurysm formation.[18] Ingebrigtsen et al[19] analyzed the vessel radii and bifurcation angles and reported that the odds ratio for aneurysm presence was 3.46 when comparing the lowest and highest tertile of the observed angle between the parent vessel and the largest branch. Sakamoto et al[20] studied the characteristics of aneurysms of the internal carotid artery (ICA) bifurcation and reported that all the ICA bifurcation aneurysms deviated to the side of the A1 segment of the anterior cerebral artery, which formed a smaller angle with the ICA than that formed between the middle cerebral artery and the ICA. Their results suggested higher hemodynamic stress experienced on the side of the A1 segment. Aneurysm formation might be related to branching characteristics that locally increase the hemodynamic stress,[21,22] and normal cerebrovascular geometry may be a risk factor in this context. The study by Rossitti and Lofgren[14] demonstrated that the branch angles of cerebral arteries may vary widely and that the apex of the bifurcation may lie in a nonoptimal position relative to the dividing streamline of the flow in the parent vessel, resulting in turbulence, vibrations, and increased shear stress on the vessel wall at the apical region, despite the fact that the blood flow/vessel radius relation is optimal.[23] The Y-stent induced angular remodeling described here effectively decreased the angle of the apex, effectively mitigating these deleterious phenomena involved in aneurysm initiation and propagation.

Meng et al[24] studied the changes in the basilar apex wall in rabbits after bilateral common carotid artery ligation and found significant internal elastic lamina (IEL) loss, media thinning, and bulge formation, with IEL loss being a prominent early change that is speculated to represent early injury that persists to become the aneurysm initiation site. Destruction of the key structural element of IEL in the vascular wall requires local matrix degradation by specialized proteolytic activity of matrix metalloproteinases. WSS is known to induce matrix metalloproteinase production by smooth muscle and endothelial cells. Consequently, the authors speculated that the unusually high WSS and the acute spatial gradient in the WSS at the basilar apex wall can stimulate overproduction of matrix metalloproteinases that degrade the IEL and other components of the extracellular matrix of the vessel wall. Further studies of the same group of authors[24,25] revealed intimal hyperplasia and matrix deposition at the apex corresponding to the flow impingement region with elevated pressure and destructive aneurysm-like remodeling (thinned vessel wall with severely disrupted IEL, reduced smooth muscle cells, and loss of endothelium, resembling early-stage intracranial aneurysms) in the acceleration region immediately adjacent to the impingement region. The WSS abruptly increased to the maximal value from the impingement center to the acceleration region but decreased gradually after entering the deceleration region further away from the impingement center. Their depiction of the impingement zone, pressure, and WSS on

Copyright © Congress of Neurological Surgeons. Unauthorized reproduction of this article is prohibited.

the basilar apex wall was similar to our findings with the maximal pressure and minimal WSS located in the impingement center and the 2 peaks of WSS just 3 mm from the impingement center. Stent struts can also change the hemodynamics in the aneurysm when a stent is deployed without coiling.[3-5] After a bifurcation aneurysm is stented coiled, the stent struts and vascular angular modification may alter the flow toward the coil mass within the aneurysm sac. Our hemodynamic analysis showed that the angular remodeling moved the peaks of WSS inward from the lateral aspects of the P1 segments of the PCA where they impinged on the vascular wall, as described by Meng et al[24], inward toward the apex where the coil mass is located, an inert nonbiologically active surface that is unlikely to be affected by the destructive remodeling process of high WSS and its spatial gradient shown in animal models of aneurysm genesis.

In the initial stage of aneurysm formation, elevated shear stress and high spatial gradients play a major role by inducing a destructive remodeling of the IEL of cerebral vessels akin to that seen in early aneurysmal formation; low shear stress does not seem to be very important in this stage.[26] However, after aneurysm formation, low shear stress can lead to further aneurysmal growth[27] and has been associated with aneurysm rupture,[28,29] possibly because low shear stress is associated with spatial disorganization of the endothelium with an assumption of a deleterious phenotype associated with decreased expression of antioxidant and anti-inflammatory mediators resulting in underlying arterial wall weakening.[30]

Blood flow at high velocities will change its momentum to static pressure when it hits the apical point of the bifurcation. With narrowing of the bifurcation angle, the incoming blood flow narrows its area of impingement on the apical point of the bifurcation, or coil mass in this study, with a resulting narrower focus of increased pressure. Given that it is the pressure that may cause a water hammer effect, leading to compression of the coil mass and possible aneurysm recurrence, the narrowing of the bifurcation angle at latest follow-up is thought to lead to a more focused pressure spot on the coil mass with sharper fall off, consequently decreasing the effect of the water hammer effect on the surrounding neck-parent vessel transition zone.

Limitations

There exist a number of limitations in the current study; some of these are related to the use of the CFD method. CFD is only as accurate as the physical models on which it is based, including the boundary conditions provided to the numerical model and the assumptions of rigid vessels lacking in radial or longitudinal viscoelasticity. We also used CFD to simulate the peak-systole state of the fluid dynamics rather than the whole cardiac cycle even though pilot studies showed peak-systole simulation to be similar to time-dependent dynamic analysis that includes the entire cardiac cycle. In addition, we assumed rigid nonslip wall conditions for the vessel wall rather than elastic wall, which would require much more complex fluid-structure interaction modeling. In this patient cohort, the elasticity of the vessel wall and its nonuniform characteristics may also have been affected by the prevailing level of atherosclerosis given the wide age range of 37 to 80 years. In addition, the study did not take into account the effect that the deployed stents would have on laminating the flow by virtue of flow deflection by their struts protruding to varying degrees into the parent vessel lumen, choosing instead to limit our attention to the dramatic angular changes that we witnessed in the analysis. Furthermore, the use of a capped configuration to simulate the complete occlusion state of the aneurysm by coil embolization may make it easier to estimate the hemodynamic alterations resulting from the angular change; however, this approach also neglects any fine changes of residual filling at the neck. Nonetheless, the goal of the study was to isolate the effect of the angular change induced by stent deployment in a Y fashion, recognizing the limitations of assuming complete embolization at the neck, as is assumed by adopting the capped configuration.

CONCLUSION

Intracranial deployment of self-expanding microstents for wide-necked aneurysms leads to a significant immediate as well as a delayed structural modification in cerebral vessel bifurcation geometry. In addition to its effects on local hemodynamics thought to be important in regulating aneurysm thrombosis and recurrence, this phenomenon needs to be taken into account when designing intracranially implanted devices with potential energy, such as self-expanding stents. Further research is needed with respect to the long-term clinical significance of the hemodynamic alterations uncovered here as a result of this novel angular remodeling phenomenon, which should be added to the other 2 known responses to intracranial stent implantation, namely, flow diversion and intimal hyperplasia.

Disclosure

Dr Malek has received unrestricted research funding from Codman Neurovascular, Stryker Neurovascular, Siemens Inc, and Microvention-Terumo for unrelated research. The other authors have no personal financial or institutional interest in any of the drugs, materials, or devices described in this article. This work was supported by a grant from the National Institutes of Health (NIH R21HL102685).

REFERENCES

1. Bendok BR, Parkinson RJ, Hage ZA, Adel JG, Gounis MJ. The effect of vascular reconstruction device-assisted coiling on packing density, effective neck coverage, and angiographic outcome: an in vitro study. *Neurosurgery*. 2007;61(4):835-840; discussion 840-841.
2. Cantón G, Levy DI, Lasheras JC. Hemodynamic changes due to stent placement in bifurcating intracranial aneurysms. *J Neurosurg*. 2005;103(1):146-155.
3. Lylyk P, Cohen JE, Ceratto R, Ferrario A, Miranda C. Endovascular reconstruction of intracranial arteries by stent placement and combined techniques. *J Neurosurg*. 2002;97(6):1306-1313.
4. Zenteno MA, Murillo-Bonilla LM, Guinto G, et al. Sole stenting bypass for the treatment of vertebral artery aneurysms: technical case report. *Neurosurgery*. 2005; 57(suppl 1):E208; discussion E208.
5. Zenteno MA, Santos-Franco JA, Freitas-Modenesi JM, et al. Use of the sole stenting technique for the management of aneurysms in the posterior circulation in a prospective series of 20 patients. *J Neurosurg*. 2008;108(6):1104-1118.

Copyright © Congress of Neurological Surgeons. Unauthorized reproduction of this article is prohibited.

6. Higashida RT, Smith W, Gress D, et al. Intravascular stent and endovascular coil placement for a ruptured fusiform aneurysm of the basilar artery. Case report and review of the literature. *J Neurosurg.* 1997;87(6):944-949.
7. Hoit DA, Malek AM. Three-dimensional rotational angiographic detection of in-stent stenosis in wide-necked aneurysms treated with a self-expanding intracranial stent. *Neurosurgery.* 2005;57(6):1228-1236; discussion 1228-1236.
8. Fiorella D, Albuquerque FC, Deshmukh VR, McDougall CG. In-stent stenosis as a delayed complication of neuroform stent-supported coil embolization of an incidental carotid terminus aneurysm. *AJNR Am J Neuroradiol.* 2004;25(10):1764-1767.
9. Fiorella D, Albuquerque FC, Woo H, Rasmussen PA, Masaryk TJ, McDougall CG. Neuroform in-stent stenosis: incidence, natural history, and treatment strategies. *Neurosurgery.* 2006;59(1):34-42; discussion 34-42.
10. Schirmer CM, Malek AM. Critical influence of framing coil orientation on intra-aneurysmal and neck region hemodynamics in a sidewall aneurysm model. *Neurosurgery.* 2010;67(6):1692-1702; discussion 1702.
11. Gao B, Baharoglu MI, Cohen AD, Malek AM. Stent-assisted coiling of intracranial bifurcation aneurysms leads to immediate and delayed intracranial vascular angle remodeling. *AJNR Am J Neuroradiol.* 2012;33(4):649-654.
12. Fiorella D, Woo HH, Albuquerque FC, Nelson PK. Definitive reconstruction of circumferential, fusiform intracranial aneurysms with the pipeline embolization device. *Neurosurgery.* 2008;62(5):1115-1120; discussion 1120-1121.
13. Hademenos GJ, Massoud TF. Biophysical mechanisms of stroke. *Stroke.* 1997;28 (10):2067-2077.
14. Rossitti S, Löfgren J. Optimality principles and flow orderliness at the branching points of cerebral arteries. *Stroke.* 1993;24(7):1029-1032.
15. Szymanski MP, Metaxa E, Meng H, Kolega J. Endothelial cell layer subjected to impinging flow mimicking the apex of an arterial bifurcation. *Ann Biomed Eng.* 2008;36(10):1681-1689.
16. Takeuchi S, Karino T. Flow patterns and distributions of fluid velocity and wall shear stress in the human internal carotid and middle cerebral arteries. *World Neurosurg.* 2010;73(3):174-185; discussion e27.
17. Roach MR, Scott S, Ferguson GG. The hemodynamic importance of the geometry of bifurcations in the circle of Willis (glass model studies). *Stroke.* 1972;3(3):255-267.
18. Brown N. A mathematical model for the formation of cerebral aneurysms. *Stroke.* 1991;22(5):619-625.
19. Ingebrigtsen T, Morgan MK, Faulder K, Ingebrigtsen L, Sparr T, Schirmer H. Bifurcation geometry and the presence of cerebral artery aneurysms. *J Neurosurg.* 2004; 101(1):108-113.
20. Sakamoto S, Kiura Y, Shibukawa M, Ohba S, Arita K, Kurisu K. Subtracted 3D CT angiography for evaluation of internal carotid artery aneurysms: comparison with conventional digital subtraction angiography. *AJNR Am J Neuroradiol.* 2006;27(6): 1332-1337.
21. Stehbens WE. Etiology of intracranial berry aneurysms. *J Neurosurg.* 1989;70(6): 823-831.
22. Steiger HJ. Pathophysiology of development and rupture of cerebral aneurysms. *Acta Neurochir Suppl (Wien).* 1990;48:1-57.
23. Rossitti S. The extreme lateral approach to thoracic disc herniations: technique and preliminary results. *Neurochirurgia (Stuttg).* 1993;36(5):161-163.
24. Meng H, Swartz DD, Wang Z, et al. A model system for mapping vascular responses to complex hemodynamics at arterial bifurcations in vivo. *Neurosurgery.* 2006;59(5):1094-1100; discussion 1100-1101.
25. Kim M, Levy EI, Meng H, Hopkins LN. Quantification of hemodynamic changes induced by virtual placement of multiple stents across a wide-necked basilar trunk aneurysm. *Neurosurgery.* 2007;61(6):1305-1312; discussion 1312-1313.
26. Meng H, Wang Z, Hoi Y, et al. Complex hemodynamics at the apex of an arterial bifurcation induces vascular remodeling resembling cerebral aneurysm initiation. *Stroke.* 2007;38(6):1924-1931.
27. Boussel L, Rayz V, McCulloch C, et al. Aneurysm growth occurs at region of low wall shear stress: patient-specific correlation of hemodynamics and growth in a longitudinal study. *Stroke.* 2008;39(11):2997-3002.
28. Shojima M, Oshima M, Takagi K, et al. Magnitude and role of wall shear stress on cerebral aneurysm: computational fluid dynamic study of 20 middle cerebral artery aneurysms. *Stroke.* 2004;35(11):2500-2505.
29. Xiang J, Natarajan SK, Tremmel M, et al. Hemodynamic-morphologic discriminants for intracranial aneurysm rupture. *Stroke.* 2011;42(1):144-152.
30. Malek AM, Alper SL, Izumo S. Hemodynamic shear stress and its role in atherosclerosis. *JAMA.* 1999;282(21):2035-2042.

COMMENTS

The authors present a very intriguing description of the effects of configurational changes in the daughter arteries secondary to the placement of intravascular stents in preparation for coiling of basilar aneurysms. In their retrospective analysis of 15 patients who underwent basilar artery aneurysm treatment with stent placement in a Y configuration and subsequent coiling the authors employ several interesting computational fluid dynamic and isolated biomorphometric analyses to describe local dynamic changes from the stenting. They note that a significant change in the P1 angles in the coronal and sagittal plane which correlated with angiographic evidence of vascular remodeling. The authors also noted that computational fluid dynamic modeling of the reconfigured arteries demonstrated a significant change in the wall shear stress and dynamic forces.

The authors present a very intriguing analysis of how complex stenting of the basilar artery changes the overall configuration of the parent and daughter vessels in this clinical scenario. There are many promising aspects to this technique and to the study of how stenting can affect vascular and aneurismal remodeling and healing. The effects observed in this clinical retrospective review are limited in similar ways to all studies of this kind. In particular, it is difficult from such observational studies to parse out the effects of angular changes of parent to daughter vessels from those of the actual presence of the stent struts. In point of fact, the geometry of the stents (open or closed cells technology) at the aneurismal ostium may have a larger effect than anticipated—an effect that cannot be modeled in this setting. The presence of the stent struts certainly alter flow dynamics within the vasculature while also altering (and slowing) flow into the aneurysm's ostium. Another significant limitation is the fact that some of the biomorphometric analyses are performed on 2-dimensional images that represent complex 3-dimensional, non-rigid structures. Indeed, some of the significant changes in angulation of P1 before and after stenting may represent a slight rotation of the images used for analysis.

A very interesting benefit that computational fluid dynamic studies (CFD) provides is the ability to assess not only wall shear stress but also dynamic forces in very specific segments. The authors describe interesting results with this respect which may in fact carry multiple interpretations. Though they suggest that a modification (or narrowing) of the bifurcation angle may cause a significant change in dynamic forces at the ostium of the aneurysm. By the studies presented, there seems to be a "focusing" of the dynamic forces along a smaller segment of the ostium. This in fact may actually be predictive of future recurrence and would be most interesting to reassess during the follow-up studies.

The authors should be commended on a well-presented study that brings to the readership some very intriguing questions in addition to interesting observations—questions that I am sure will be addressed in future studies.

Charles J. Prestigiacomo
Newark, New Jersey

Based on technical difficulties, complications, mass effect concerns, and recurrence associated with coiling of wide necked aneurysms, an interest grew in the use of stents as an adjunct or even standalone treatment for intracranial aneurysms.[1-4] Early on, a hemodynamic effect of stenting was noted on aneurysms.[5] In addition to the hemodynamic effects, stenting has been shown to impact coil mass features which may have an impact on durability of treatment.[6] Growing evidence supports an association between stenting and durability of treatment.[7,8] Hemodynamic studies have suggested a strong correlation between parent artery

Copyright © Congress of Neurological Surgeons. Unauthorized reproduction of this article is prohibited.

curvature and hemodynamics within an aneurysm.[9,10] While it appears plausible that variations in parent artery curvature, with a resulting variation in inflow angle, would have an effect on aneurysm behavior, it is not clear weather altering these parameters could have a positive or deleterious effect on aneurysm natural history.

In this paper, the authors report on the geometric and potential hemodynamic effects of Y-stenting of basilar apex aneurysms in 15 patients. The authors measured the impact of stenting on the following angles: the angle between the proximal P1 segments, and the angles between the P1s and the basilar artery in both the sagittal and coronal planes. They utilized computational fluid dynamic studies (CFD) to analyze the hemodynamic effects of the angular changes imposed by stenting on the treated of aneurysms and the coil masses within them. Stenting decreased the angle between the 2 P1s resulting in an increase in the angle between the P1s and basilar artery in the coronal plane. The angles between the P1s and the basilar artery were decreased in the sagittal plane. These changes were noted to have progressed on follow up imaging. Using CFD, the authors found that these geometric changes may have shifted high wall shear stress away from the aneurysm neck transition zone to the coil mass. The authors hypothesize that this possible shift would have a beneficial effect on durability of treatment. The findings of this study are very interesting but the ability to translate CFD findings to actual in vivo hemodynamics remains limited. Clinical (in vivo) validation of the authors' findings is needed before the results can be used to justify an alteration in clinical practice. A number of questions are raised by this study: (1) does the shift of hemodynamic stress to the coil mass away from the original inflow zone positively or negatively affect recurrence? While the coil mass is "inert" biologically when first placed, it quickly becomes a dynamic structure from biophysical and biological standpoints. Coil masses can remodel over time and serve as lattices for biological activity. (2) Is Y-stenting justified based on hemodynamic considerations alone? In my experience, a single stent (from basilar artery to the more cranial P1 or from P1 to P1) is very effective in the vast majority of cases when stenting is needed for wide necked basilar apex aneurysms. Whether Y-stenting is more effective than this at reducing recurrence and improving overall results remains unclear. The additional potential acute and delayed risks of adding a second stent should be carefully considered. (3) How can these results be further validated? Modern MRI techniques hold great promise as a tool to study aneurysm hemodynamics in vivo.[11] Ultimately, more clinical studies which address long term outcome are needed to help shed light on best approaches for basilar apex aneurysms.

The authors are to be congratulated on looking beyond the surface on the issue of Y-stent assisted coiling and raising several interesting hypotheses that should be the focus of further investigation. As the number of techniques and devices for intracranial aneurysms grows, comparative effectiveness research will be needed to shed light on which approaches will lead to the best short and long term outcomes.

Bernard R. Bendok
Tarek Y. El Ahmadieh
Najib E. El Tecle
Timothy R. Smith
Chicago, Illinois

1. Xu DS, Hurley MC, Batjer HH, Bendok BR. Delayed cranial nerve palsy after coiling of carotid cavernous sinus aneurysms: case report. *Neurosurgery.* 2010;66(6): E1215-E1216.
2. Mericle RA, Lanzino G, Wakhloo AK, Guterman LR, Hopkins LN. Stenting and secondary coiling of intracranial internal carotid artery aneurysm: technical case report. *Neurosurgery.* 1998;43(5):1229-1234.
3. Szikora I, Guterman LR, Wells KM, Hopkins LN. Combined use of stents and coils to treat experimental wide-necked carotid aneurysms: preliminary results. *AJNR. American journal of neuroradiology.* 1994;15(6):1091-1102.
4. Wakhloo AK, Lanzino G, Lieber BB, Hopkins LN. Stents for intracranial aneurysms: the beginning of a new endovascular era? *Neurosurgery.* 1998;43(2): 377-379.
5. Lieber BB, Livescu V, Hopkins LN, Wakhloo AK. Particle image velocimetry assessment of stent design influence on intra-aneurysmal flow. *Annals of biomedical engineering.* 2002;30(6):768-777.
6. Bendok BR, Parkinson RJ, Hage ZA, Adel JG, Gounis MJ. The effect of vascular reconstruction device-assisted coiling on packing density, effective neck coverage, and angiographic outcome: an in vitro study. *Neurosurgery.* 2007;61(4):835-840; discussion 840-831.
7. Chalouhi N, Dumont AS, Hasan D, et al. Is packing density important in stent-assisted coiling? *Neurosurgery.* 2012;71(2):381-386; discussion 386-387.
8. Mocco J, Snyder KV, Albuquerque FC, et al. Treatment of intracranial aneurysms with the Enterprise stent: a multicenter registry. *Journal of neurosurgery.* 2009;110 (1):35-39.
9. Hoi Y, Meng H, Woodward SH, et al. Effects of arterial geometry on aneurysm growth: three-dimensional computational fluid dynamics study. *Journal of neurosurgery.* 2004;101(4):676-681.
10. Meng H, Wang Z, Kim M, Ecker RD, Hopkins LN. Saccular aneurysms on straight and curved vessels are subject to different hemodynamics: implications of intravascular stenting. *AJNR. American journal of neuroradiology.* 2006;27(9): 1861-1865.
11. Frydrychowicz A, Markl M, Harloff A, et al. [Flow-sensitive in-vivo 4D MR imaging at 3T for the analysis of aortic hemodynamics and derived vessel wall parameters]. *RoFo: Fortschritte auf dem Gebiete der Rontgenstrahlen und der Nuklearmedizin.* 2007;179(5):463-472.

Copyright © Congress of Neurological Surgeons. Unauthorized reproduction of this article is prohibited.